BIBECHANA
Vol. 23, No. 2, April 2026, 1–8

ISSN 2091-0762 (Print), 2382-5340 (Online)
Journal homepage: http://nepjol.info/index.php/BIBECHANA
Publisher:Dept. of Phys., Mahendra Morang A. M. Campus (Tribhuvan University)Biratnagar

Stress transfer using the Okada dislocation model: A case study of the Gorkha Earthquake

Eak Raj Paudel[1,2*], Ram Krishna Tiwari[2*], Uday Bahadur Thapa Kshetri[1,2], Rudra Prasad Poudel[1,2], Harihar Paudyal[2]

[1]*Central Department of Physics, Tribhuvan University, Kirtipur, Kathmandu, Nepal.*
[2]*Birendra Multiple Campus, Tribhuvan University, Bharatpur, Nepal.*

[*]Corresponding authors: Email: eak.poudel@bimc.tu.edu.np;ram.tiwari@bimc.tu.edu.np

Abstract

Static Coulomb stress change (ΔCFS) plays a major role in earthquake triggering and seismic hazard assessment in tectonically active regions like the Central Himalaya. We investigate ΔCFS produced by the 2015 Gorkha earthquake using a rectangular fault model and the Okada (1992) elastic dislocation solution in a homogeneous, isotropic half-space. Five slip scenarios (2.0–6.5 m) are evaluated and stress fields are analyzed through 1D profiles and 2D spatial mapping. The results show that ΔCFS increases linearly with slip amplitude, with higher slip producing stronger stress concentration near the rupture zone. A strong linear scaling between slip and peak stress is observed, with each meter of slip contributing approximately 2.13 MPa. The 2D stress maps reveal symmetric positive and negative lobes around the rupture, with stress decaying rapidly with distance. The longitudinal stress profiles demonstrate a sharp concentration of stress at the epicenter (28.147°N, 84.708°E), with symmetric decay to near-zero levels within about $\pm 1.3°$ longitude. These findings indicate that slip amplitude primarily governs local stress concentration with short-range triggering potential, while far-field stress patterns are comparatively insensitive to variations in slip magnitude. This study emphasizes the importance of ΔCFS analysis in understanding stress transfer mechanisms and assessing post-seismic hazard in complex tectonic regions.

Keywords
Coulomb stress, elastic rebound theory, slip, fault, Himalaya seismicity.

Article information
Manuscript received: October 3, 2025; Revised: April 17, 2026; Accepted: April 21, 2026
DOI: https://doi.org/10.3126/bibechana.v23i2.85018

1 Introduction

The Gorkha Earthquake 2015 (M_w 7.8) struck central Nepal on 25 April 2015, followed by a strong aftershock sequence [1]. The epicenter was located near Gorkha, approximately 80 km northwest of Kathmandu, and ruptured a ∼150 km segment of the Main Himalayan Thrust (MHT) beneath the

central Himalaya [2]. The earthquake resulted from long-term stress accumulation due to the ongoing convergence (∼17–21 mm/yr) between the Indian Plate and the Eurasian Plate, leading to the sudden release of strain along a shallowly dipping thrust fault [3].

The phenomenon of earthquake occurrence has undergone a significant conceptual evolution over the past century. Initially, it is viewed as isolated geophysical events caused by localized stress accumulation hence failure. Modern seismology now recognizes earthquakes as part of a larger, interconnected stress field. One rupture can influence the timing and location of others. The foundation of this understanding based on Reid's elastic rebound theory [4], which postulated that tectonic stress builds gradually along a fault and is released suddenly during rupture, returning the system to a stress-free state. While this model explained the mechanics of individual earthquakes, it did not consider how one earthquake might affect other faults spatially and temporally. A major leap forward came with the work of Scholz [5], who emphasized the role of fault segmentation, stress heterogeneity, and fault mechanics in understanding earthquake triggering. The contributions generate the idea that faults do not behave in isolation but influence one another through stress changes. The concept of Coulomb stress transfer was formalized by King, Stein and Lin [6]. It is proposed that earthquakes not only relieve stress but also redistribute it across nearby faults. This redistribution can either promote or inhibit rupture on neighboring segments. The stress change is quantified by the Coulomb Failure Stress Change ΔCFS [7], defined as

$$\Delta CFS(\sigma_f) = \Delta\tau + \mu'\Delta\sigma_n \quad (1)$$

Here, $\Delta\tau$ be the change in shear stress on the fault and $\Delta\sigma_n$ be the change in normal stress on the fault. Similarly, μ' be the effective frictional coefficient having value 0.2-0.8. Simply it is used to evaluate how slip on one fault could promote or inhibit failure on nearby faults. A positive ΔCFS brings a fault closer to failure, increasing the likelihood of triggering aftershocks or subsequent earthquakes, whereas a negative ΔCFS indicates stress shadowing and stabilization.

To better understand the relationship between stress components and failure potential, we refer to the Mohr–Coulomb failure criterion, graphically depicted in Figure 1. This diagram explains how the failure of faults is accountable on the scale between shear stress and effective normal stress acting on fault planes. The red failure envelope separates stable from unstable regions in stress space, which highlights the geometry of a fault plane under stress orientation [8].

Following the initial formulation, Dieterich [9] introduced rate-and-state friction laws, which provided a dynamic model of how stress influences earthquake probability. The Dieterich's work showed that even minor changes in ΔCFS could cause statistically significant changes in seismicity rates, thus strengthening the Coulomb framework's physical basis. A critical assessment of stress transfer models was carried out by Harris [7], who warned that despite the utility of ΔCFS models, uncertainties in fault geometry, slip distribution and regional stress fields could introduce significant errors. This work emphasized that Coulomb stress models are better suited for retrospective analysis than deterministic prediction, yet they remain crucial for seismic hazard mapping. Recent studies [10] have reaffirmed the shift from viewing earthquakes as isolated events to seeing them as parts of complex fault networks, interconnected through stress transfer processes. This networked view of seismicity underscores the importance of understanding how a single rupture can influence the broader tectonic system [11].

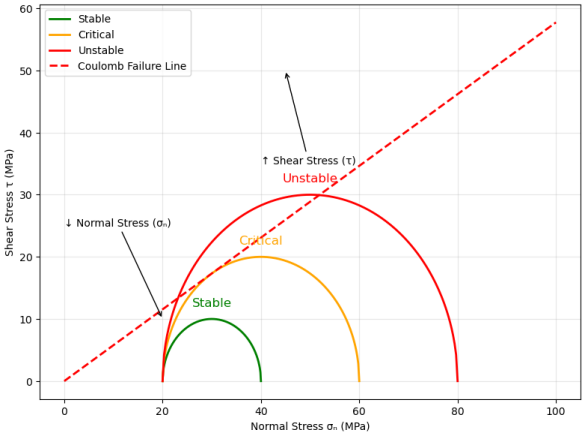

Figure 1: Mohr circle and stability curve under stress.

1.1 Broader ideas and contemporary debates

The Coulomb stress transfer model remains leading in seismology. Many recent studies have offered nuanced views and critical assessments that enrich our understanding of its applicability and limitations. Empirical analysis [12] found robust statistical support for static triggering in Southern California catalogues. Authors found that stress changes as small as ∼ 10 Pa can correlate with increased seismicity. It is also noted that predictive power decays within a few hundred days due to the loss of "stress memory" in the crust. Similarly, other researchers

have highlighted shortcomings of the static model. The Researcher also found that aftershock rates are lower in stress shadows regions [7]. However, the seismicity in those areas does not fall below the normal background level. This may be due to dynamic triggering. It is about 34% of aftershocks may be caused by dynamic stress changes, not just static stress transfer [13]. In another review [14] noted that stress transfer is important for understanding how earthquakes interact. Many factors, such as variations in the crust, changes in pore pressure, fluid–rock interactions, and limitations of the old Volterra model [15], can strongly affect ΔCFS. In conclusion, Coulomb stress transfer provides useful insight, but it should be combined with other models such as dynamic triggering and aseismic processes.

In this study, we simulate Coulomb stress change patterns generated by a simplified main shock scenario using a rectangular fault model in a homogeneous elastic half-space. The Okada elastic dislocation solution [16] is applied to compute ΔCFS across a spatial 2D grid, enabling the identification of stress loading and shadow zones around the rupture. Modeled results will be compared with observed secondary earthquake data to validate the approach. This work highlights how a single rupture can redistribute stress in the surrounding crust, providing insights into earthquake triggering processes.

2 Methods and methodology

2.1 Theoretical and mathematical framework

The Okada dislocation mode [16] provides an analytical formulation to estimate surface deformation and stress field changes due to fault slip within a homogenous, elastic half-space. In this model, an earthquake rupture is idealized as a rectangular fault plane, and the surrounding earth is treated as a linearly elastic and isotropic medium. The model is based on the theory of Volterra dislocations [15], where discontinuities in displacement produce strain fields in the surrounding material.

Point source model (top): In this method, the fault is represented as a single source point defined by depth, dip and the observer location (X, Y, Z). This simplified approach approximates the earthquake as a concentrated slip at depth (Figure 2).

Rectangular fault source model (bottom): In this model, the fault is represented as a finite rectangular plane with dimensions (AL1, AL2, AW1 and AW2), dip and depth. The slip vector is decomposed into three components (DISL1: strike-slip, DISL2: dip-slip, DISL3: tensile component). The observer point (X, Y, and Z) measures the resulting deformation, making this model more realistic for analyzing static stress transfer and fault mechanics, Figure 2.

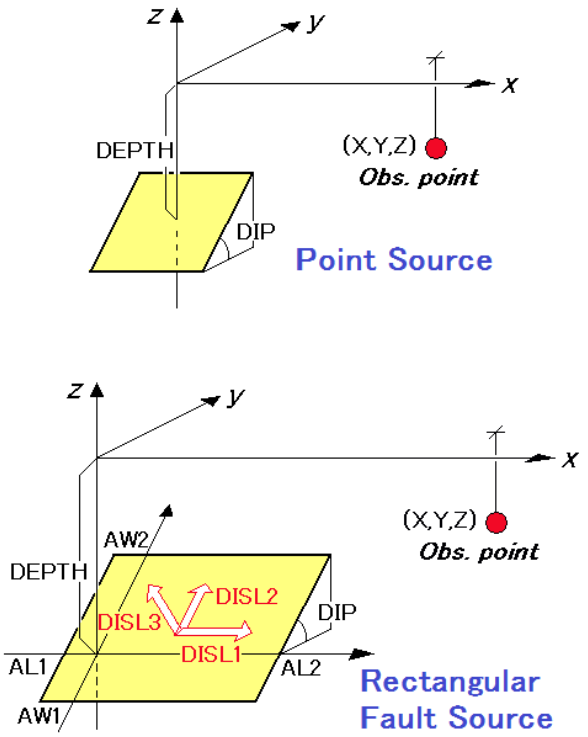

Figure 2: Schematic representation of earthquake source models used in Coulomb stress and displacement calculations [16].

When a fault slips, it not only releases strain energy but also redistributes stress in the crust. The Okada solution analytically solves Navier's equations of elasticity for this scenario using the parameters such as fault length (L), width (W), depth to the top edge including strike, dip, rake, and amount of slip (d) of the fault.

In this study, we simplify the model by considering a 2D vertical fault aligned along the x-axis and evaluate stress at surface points located horizontally from the rupture center. The components of stress are given as [17, 18]

$$\Delta\tau = \frac{\mu.d.L}{2\pi r^2} \tag{2}$$

$$\Delta\sigma_n = \frac{\mu.d.W}{2\pi r^2} \tag{3}$$

where μ is the shear modulus of the Earth's crust and r is the radial distance from the fault center.

2.2 Computational framework

In this study, the Okada equations were implemented in a FORTRAN to compute $\Delta\tau$ (Change in shear stress), $\Delta\sigma_n$ (change in normal stress) and ΔCFS at surface grid points using the parameters from Table 1. The fault is assumed to be vertical (dip = 90°) with a strike of 0° and pure thrust motion (rake = 90°), having a length of 120 km and a down-dip width of 60 km, with its top located at 15 km depth. Five slip scenarios (2.0, 3.0, 5.0, 6.0, and 6.5 m) were used to investigate the influence of slip amplitude on stress transfer. The surrounding crust is represented by a homogeneous, isotropic half-space with a shear modulus of 30 GPa and an effective friction coefficient of 0.4, consistent with the assumptions of the Okada dislocation model and a traction-free surface boundary condition. The effects of material heterogeneity, layered crustal structure and complex fault geometry are not included in this formulation. Coulomb stress change was computed along a 1D profile extending from −200 km to 200 km along strike, with near-field smoothing applied at distances less than 1 km. The computational grid was discretized with uniform spatial spacing. The stress components were evaluated as a function of radial distance from the fault center. The order of magnitude of the computed Coulomb stress changes is consistent with values reported in previous earthquake studies confirming the physical reliability of the results. This framework allowed us to systematically explore the spatial pattern of stress transfer associated with varying slip amplitude. Post–processing and plotting were performed in Python, generating line profiles of ΔCFS versus horizontal distance and 2D maps of stress increase and shadow zones.

Table 1: Parameters used in the study

Parameters	Value	Description	References
μ (GPa)	30.0×10^9	Shear modulus of crustal rocks	[19]
μ'_{eff}	0.4	Effective friction coefficient	[6, 20]
L (km)	120.0	Fault length along strike	[19, 20]
W (km)	60.0	Fault width down depth	[19]
H (km)	15	Depth from epicenter	USGS
S_1 (m)	2.0	Slip for heterogeneous multi-patch simulation	[21]
S_2 (m)	3.0	Lower-bound slip for sensitivity tests	Small-slip inversion cases
S_3 (m)	5.0	Moderate slip from finite fault inversion	[19]
S_4 (m)	6.0	Representative average slip in main rupture patch	[10, 19]
S_5 (m)	6.5	Peak slip in high-slip subpatches	Field and inversion extremes

3 Results and discussion

In this section, we have analyzed the slip dependency of ΔCFS by computational approaches using tools like FORTRAN and Python. Figure 3 shows the line profiles of ΔCES versus distance, with a narrow peak centered at the rupture (0 km) for all slip scenarios. Peak ΔCES scales with slip magnitude: the highest-slip case (S5 = 6.55 m) produces the largest peak, while low–slip cases S1 (2.0 m) and S2 (3.0 m) display substantially reduced central peaks. The stress field is nearly symmetric about the rupture center. All scenarios display a steep gradient within the first 30–50 km and approach near–zero perturbation beyond ∼100 km.

Coulomb stress transfer during the Gorkha earthquake is strongly controlled by slip order. The stress field shows a symmetric distribution about the rupture zone, with peak ΔCFS concentrated near the fault. The observed stress range (∼4–13 MPa) and its inverse-distance decay are in agreement with theoretical predictions and previous studies based on the Okada formulation [16] and Coulomb stress transfer theory [22]. The observed value of stress change (4–13 MPa) in this study is in agreement with the ∼7 MPa lower bound of the energy–based average stress drop reported for the Gorkha earthquake [23]. This confirms that the co-seismic stress drop occurs on the source fault rather than through far-field stress transfer.

Similar stress magnitudes and spatial patterns have been reported for the 2015 Gorkha earthquake, where positive Coulomb stress changes were found to correlate with aftershock distribution and stress loading on adjacent fault segments [24]. The linear scaling relationship between slip and peak stress further confirms that slip amplitude is the dominant factor governing co–seismic stress redistribution, consistent with elastic dislocation theory. This behavior follows from linear elastic dislocation theory, where stress perturbations are proportional to fault slip [25].

The graph below (in Figure 4 (a,b)) shows the comparison of stress order for different slip values, indicating variation in the stress profile from 4 MPa to 13 MPa.

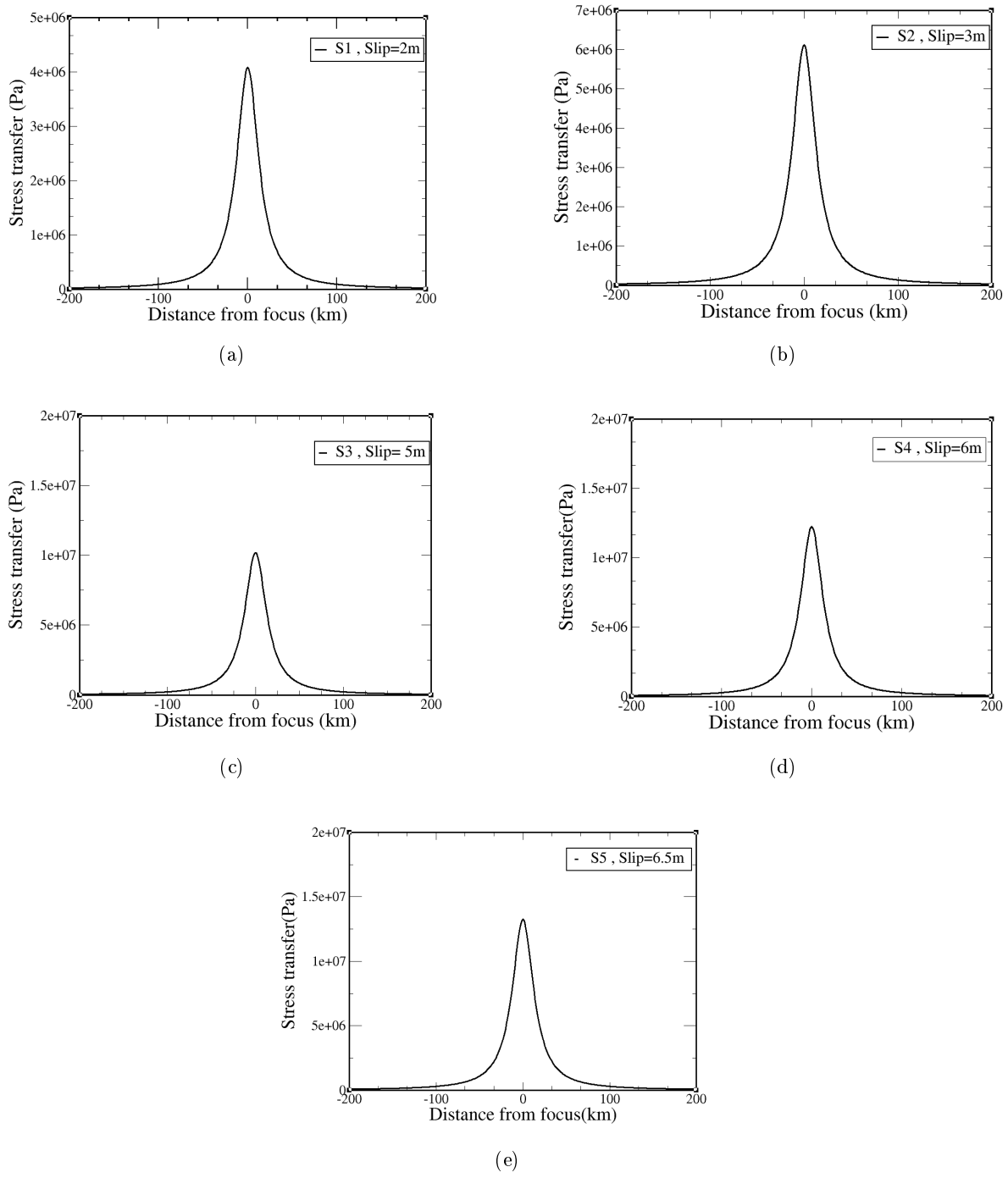

Figure 3: Coulomb stress change for different slip scenarios using FORTRAN (S1–S5).

Figure 4(a) shows the variation of Coulomb stress change (ΔCFS) with distance from the fault epicenter, showing a sharp peak at the rupture zone (x = 0 km), where maximum stress values reach ∼4–13 MPa depending on slip amplitude (2–6.5 m). The distribution is nearly symmetric about the epicenter and decays rapidly with distance, approximately following a $1/r^2$ trend, becoming negligible beyond 100–200 km. While larger slip models produce proportionally higher peak stresses near the fault, the curves converge at greater distances, indicating that slip strongly influences local stress redistribution but has minimal regional effect. This pattern highlights how earthquakes concentrate stress near the rupture zone, with implications for aftershock triggering and secondary fault activation.

Figure 4(b) shows the variation of Coulomb stress

change (ΔCFS) along longitude for different slip models. The stress is maximum at the epicenter (28.147° N, 84.708° E, where the earthquake rupture initiated and gradually decays in both eastward and westward directions.

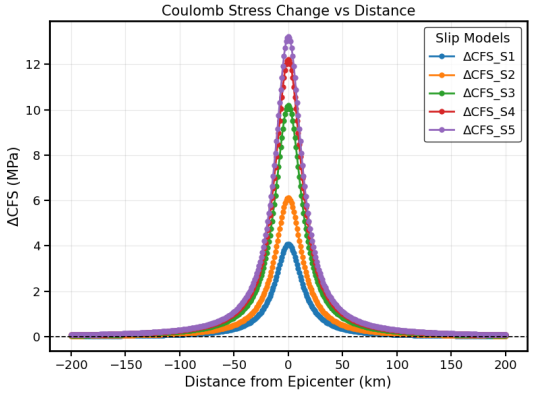

(a)

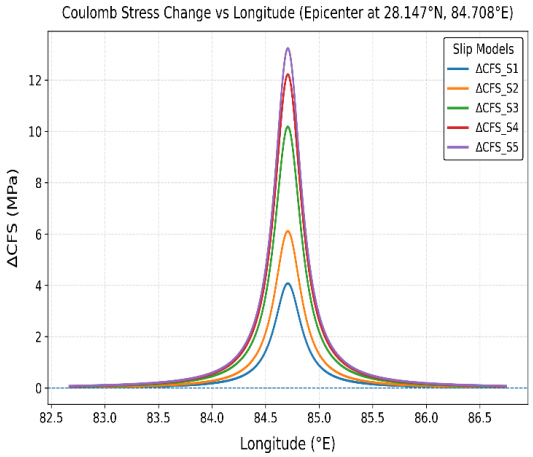

(b)

Figure 4: (a) Comparison of stress transfer by distance (b) longitudinal variation of stress transfer).

The map profile (Figure 5) shows an elliptical concentration of positive stress near the epicenter, with peak values increasing with slip. Stress perturbations decay outward significantly after 20 km, consistent with the localized nature of co–seismic stress changes observed in the 1D profiles.

The plot illustrates the relationship between maximum Coulomb stress change (ΔCFS) and fault slip, revealing a strong linear trend, Figure 6. As slip increases from 2.0 to 6.5 m, the peak stress also rises nearly proportionally. The regression analysis yields the best-fit line

$$\text{Stress} = 2.13 * \text{Slip} + 0.26 \quad (4)$$

with a regression coefficient $R^2 = 0.92$, indicating an excellent fit.

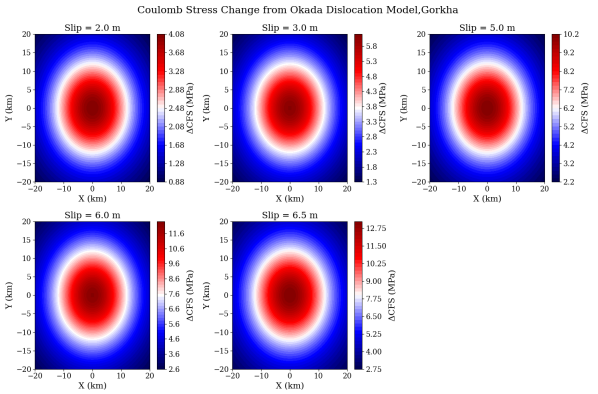

Figure 5: Coulomb stress change (ΔCFS) distributions for the Gorkha scenario with slip amplitudes of 2.0–6.5 m.

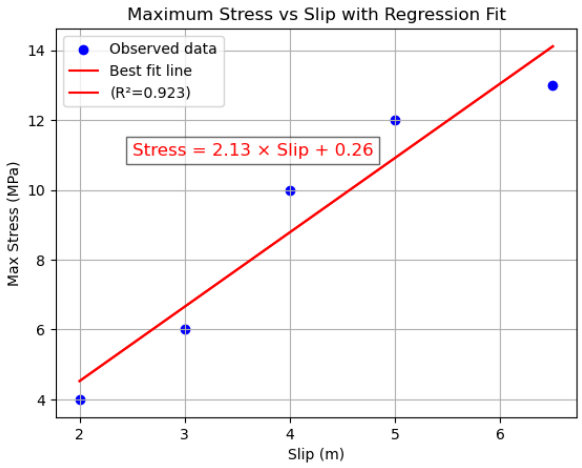

Figure 6: Variation of maximum stress with respect to slip on a fault.

The slope (∼2.13 MPa/m) suggests that each additional meter of slip contributes approximately 2.13 MPa of peak stress increase, Figure 6. The small positive intercept reflects negligible stress in the absence of slip, which aligns with theoretical expectations. This finding is consistent with elastic dislocation theory by Okoda [16], which predicts that Coulomb stress changes scale linearly with slip amplitude for a fixed geometry and elastic medium. Earlier studies also emphasized that stress perturbations increase proportionally with fault slip, typically ranging from a few tenths to several MPa per meter depending on fault orientation and crustal properties [19]. The results here confirm this scaling, showing that stress transfer is dominantly controlled by slip amplitude, with model-specific parameters influencing the exact slope. Thus, the regression provides strong support for the theoretical framework that fault slip is the primary driver of co–seismic stress redistribution.

The present model assumes a simplified homogeneous medium and uniform slip distribution, which may not fully capture the complexity of real fault geometry and crustal heterogeneity in the Himalayan region. Despite these limitations, the results provide a physically consistent representation of stress transfer, regional seismicity [26], and offer useful insights into stress accumulation and seismic hazard after large earthquakes like the 2015 Gorkha earthquake.

4 Conclusion

The modeled ΔCFS patterns show that slip magnitude is the dominant control on near-field stress amplitude. Higher slip increases local Coulomb stress and creates larger loading areas that may promote aftershocks on nearby fault patches. However, all slip models predict a similar spatial decay of static stress change, with negligible perturbation beyond ∼100 km from the rupture. This indicates that the main impact of slip variability is confined to the rupture vicinity, while far–field regions are less sensitive to slip differences. The regression analysis further confirms a robust linear relationship between slip and peak stress (Stress $= 2.13 * \text{Slip} + 0.26$), supporting the theoretical expectation that static stress transfer scales directly with fault slip. These results highlight that static Coulomb stress analysis is a useful diagnostic for identifying regions of enhanced or reduced failure potential but its quantitative predictive power depends critically on accurate slip distributions, receiver-fault orientations and incorporation of additional processes such as pore-fluid pressure, viscoelastic relaxation, and dynamic stress changes. Overall, the study highlights both the strengths and the limitations of the ΔCFS approach in Seismology.

Acknowledgements

First author would like to express my sincere gratitude to the Institute of Science and Technology (IoST) and the Central Department of Physics, Tribhuvan University (TU), for providing the academic platform and support to carry out my Ph.D. study. I am also thankful to Birendra Multiple Campus for granting study leave, which has enabled me to focus on the research. Their encouragement and assistance have been invaluable in the successful completion of this work.

References

[1] Tiwari RK, Paudyal H. Gorkha earthquake (Mw 7.8) and aftershock sequence: A fractal approach. Earthquake Science. 2022;35(3):193-204.

[2] Kumar A, Singh SK, Mitra S, Priestley KF, Dayal S. The 2015 April 25 Gorkha (Nepal) earthquake and its aftershocks. Geophysical Journal International. 2017;208(2):992-1008.

[3] Ader T, Avouac JP, Liu-Zeng J, Lyon-Caen H, Bollinger L, Galetzka J, et al. Convergence rate across the Nepal Himalaya and interseismic coupling on the Main Himalayan Thrust: Implications for seismic hazard. Journal of Geophysical Research: Solid Earth. 2012;117(4):1-16.

[4] Reid HF. The California Earthquake of April 18, 1906. Carnegie Institution of Washington; 1910.

[5] Scholz CH. The Correspondence of Earthquakes and Faults. 2025.

[6] Stein S. Static stress changes and the triggering of earthquakes. Bulletin of the Seismological Society of America. 1994;84(3):935-53.

[7] Harris RA. Introduction to special section: Stress triggers, stress shadows, and implications for seismic hazard. Journal of Geophysical Research: Solid Earth. 1998;103(10):24347-58.

[8] Dahm T, Hainzl S. A Coulomb Stress Response Model for Time-Dependent Earthquake Forecasts. Journal of Geophysical Research: Solid Earth. 2022;127(9).

[9] Dieterich JH. A constitutive law for rate of earthquake production. Journal of Geophysical Research: Solid Earth. 1994;99:2601-18.

[10] Duan H, Wu S, Kang M, Xie L, Chen L. Fault slip distribution of the 2015 Mw7.8 Gorkha (Nepal) earthquake estimated from InSAR and GPS measurements. Journal of Geodynamics. 2020;139:101767.

[11] Foulger GR, Wilson MP, Gluyas JG, Julian BR, Davies RJ. Global review of human-induced earthquakes. Earth-Science Reviews. 2018;178:438-514.

[12] Nandan S, Ouillon G, Woessner J, Sornette D, Wiemer S. Earthquake triggering models. Journal of Geophysical Research: Solid Earth. 2016:1890-909.

[13] Hardebeck JL, Harris RA. Stress based earthquake triggering models. Journal of Geophysical Research: Solid Earth. 2022;127.

[14] Qi C. Dynamically triggered seismicity on a tectonic scale: A review. 2024.

[15] Volterra V. Elastic equilibrium theory. Annales Scientifiques de l'École Normale Supérieure. 1907;24:401-517.

[16] Okada Y. Internal deformation due to shear and tensile faults in a half-space. Bulletin of the Seismological Society of America. 1992;82(2):1018-40.

[17] Segall P, Laws C. Earthquake and Volcano Deformation. Princeton University Press; 2008.

[18] Okada Y. Surface deformation due to shear and tensile faults in a half-space. Bulletin of the Seismological Society of America. 1985;75(4):1135-54.

[19] Galetzka J, Melgar D, Genrich JF, Geng J, Owen S, Lindsey EO, et al. Slip pulse and resonance of the Kathmandu basin during the 2015 Gorkha earthquake, Nepal. Science. 2015;349(6252):1091-6.

[20] Freed AM. Earthquake triggering by static stress transfer. Annual Review of Earth and Planetary Sciences. 2005;33:335-67.

[21] Tung S, Masterlark T. Earthquake deformation analysis. Journal of Geophysical Research: Solid Earth. 2016:3479-503.

[22] King G, Stein RS, Lin J. Static stress changes and the triggering of earthquakes. Bulletin of the Seismological Society of America. 1994;84(3).

[23] Adams M, Hao J, Ji C. Energy-based average stress drop and its uncertainty during the 2015 M w 7.8 Nepal earthquake constrained by geodetic data and its implications to earthquake dynamics. Geophysical Journal International. 2019;217(2):784-97.

[24] Chan CH, Wang Y, Almeida R, Yadav RBS. Enhanced stress and changes to regional seismicity due to the 2015 Mw 7.8 Gorkha, Nepal, earthquake. Journal of Asian Earth Sciences. 2017;133:46-55.

[25] Aki K, Richards P. Quantitative Seismology. University Science Books; 2002.

[26] Reasenberg PA, Simpson RW. Response of regional seismicity to the static stress change produced by the Loma Prieta earthquake. Science. 1992;255(5052):1687-90.